ELSEVIER

Polymer Vol. 37 No. 13, pp. 2831–2844, 1996

0032-3861/96/$15.00+0.00

Monte Carlo simulation of network formation based on structural fragments in epoxy–anhydride systems

Umang Khanna and Manas Chanda*
Department of Chemical Engineering, Indian Institute of Science, Bangalore 560 012, India
(Received 15 February 1995; revised 6 November 1995)

A method combining the Monte Carlo technique and the simple fragment approach has been developed for simulating network formation in amine-catalysed epoxy–anhydride systems. The method affords a detailed insight into the nature and composition of the network, showing the distribution of various fragments. It has been used to characterize the network formation in the reaction of the diglycidyl ester of isophthalic acid with hexahydrophthalic anhydride, catalysed by benzyldimethylamine. Pre-gel properties like number and weight distributions and average molecular weights have been calculated as a function of epoxy conversion, leading to a prediction of the gel-point conversion. Analysis of the simulated network further yields other characteristic properties such as concentration of crosslink points, distribution and concentration of elastically active chains, average molecular weight between crosslinks, sol content and mass fraction of pendent chains. A comparison has been made of the properties obtained through simulation with those predicted by the fragment approach alone, which, however, gives only average properties. The Monte Carlo simulation results clearly show that loops and other cyclic structures occur in the gel. This may account for the differences observed between the results of the simulation and the fragment model in the post-gel phase.

(Keywords: Monte Carlo simulation; epoxy–anhydride; structural fragments)

INTRODUCTION

The network build-up in the stepwise polymerization of polyfunctional monomers is of great interest for the understanding and prediction of properties that are related to the development of network structures, such as viscosity, gel point and crosslinking, and also the final properties of the network, like modulus, damping, ultimate strength, permeability, etc. The ability to predict the network structure, given the starting monomers and process conditions, is indeed valuable.

The gel point is probably the most important molecular parameter to evaluate for a network polymerization. Flory[1] and Stockmayer[2] laid out the basic relations between extent of reaction and resulting structure in non-linear polymerization, particularly for the extent of polymerization at the gel point, p_{gel}. For reaction extents greater than p_{gel}, an infinite network exists and the sample is like a solid. Flory[1] and Stockmayer[2] in a more general way calculated the distribution of molecular weights that arises during stepwise polymerization. Starting with the assumptions of equal reactivity of functional groups and no intermolecular reactions, they used combinatorial methods to derive expressions for the size distribution of the finite molecules as a function of the extent of reaction. For cases of practical importance, however, these distribution functions become quite complex[3] and difficult to use.

Gordon[4] showed that the molecular-weight averages could be calculated directly using the theory of stochastic branching processes[5]. He and his coworkers have used this approach extensively to calculate a number of network structural relations[6–10]. Gordon's technique involves abstract mathematics and requires deriving vector probability generating functions[4].

Although Gordon's method is quite general, it has not been widely applied to network problems as it is rather difficult to use. It requires breaking down of the reactive monomers somewhat artificially and usually yields equations in matrix form. Dušek and coworkers[11] used this approach for analysing epoxy–amine networks. The method involves transformation of the branching process into the growth of probability trees[12]. An assembly of all realizable probability trees (*statistical forest*) is considered as a graphical-theoretical representation of the existing molecular formations.

A simpler method of developing property relations for non-linear systems was presented by Macosko and Miller[13]. Compared to the earlier methods of Flory and Stockmayer, which first calculate the distribution of all species and then use the distribution to calculate average properties, the method of Macosko and Miller[13], based on expectation theory, calculates these properties directly. In contrast to the method of Gordon, it does not require probability generating functions. Bokare and Gandhi[14] combined the relatively simple concepts of expectation theory developed by Macosko and Miller with a kinetic model accounting for the generation of epoxy–amine clusters to treat epoxide curing with

* To whom correspondence should be addressed

amines. They used this approach to study the effect of simultaneous etherification reaction on epoxy–amine curing. They studied the influence of epoxy–amine stoichiometric ratios and rate-constant ratios on the weight-average molecular weight and the gelation condition.

Essentially the same approach was used by Dušek[15], who, however, applied a cascade method to kinetically generated clusters (amine–polyepoxy adducts) to evolve a theoretical treatment of network formation in diamine–diepoxide curing with etherification of the excess epoxide groups. Although the model is applicable to general calculations of statistical parameters in both pre-gel and post-gel stages, only the effect of etherification reaction on the gelation condition was analysed.

Dušek and Šomvársky[16] have shown that the application of a branching theory based on statistical (Markovian) network build-up from units is not rigorous. In the case of initiated polyreactions, as in epoxy curing, it may lead to large deviations from the current solution obtained by the kinetic method. Thus, for an initiated living polymerization process, the gel-point conversion was shown[16] to be larger by up to 50% compared to the approximate statistical build-up from units. The reason for divergence of the results obtained by statistical and kinetic methods is that the statistical generation from units is always a Markovian process, yielding a Markovian distribution of the degree of polymerization, while the kinetic process is described by an infinite set of deterministic differential equations of chemical kinetics, which yield a non-Markovian distribution.

In the statistical structural model (SSM) developed by Riccardi and Williams[17], the network is built up from structural fragments larger than monomer units and the fragment distribution is obtained by solving a finite number of differential equations based on chemical kinetics. Using this approach expressions were derived for the number- and weight-average molecular weights, gel-point conversion, sol fraction, mass fraction of pendent chains and concentration of elastically active network chains.

In summary, there are thus three different approaches to generate statistical parameters: (i) statistics applied to initial molecules (monomers) using probability theory; (ii) statistics applied to kinetically generated clusters; and (iii) statistics applied to kinetically generated fragments (SSM).

Though the fragment model of Riccardi and Williams[17] is less rigorous than the methods using distribution functions, its results compare quite well with those obtained by Dušek's cluster approach[15]. However, the fragment model only predicts average properties and is unable to provide number- and weight-fraction distributions or any other information that can be derived only by examining the composition of the network, e.g. the longest chain in the network, nature of a crosslink, molecular weight between crosslinks. Such detailed information provides further insight into the structural characteristics of the network and hence into the structure–property relations.

Monte Carlo simulation techniques have been extensively used in many contexts[18], including coupled chemical reactions[19], molecular-weight distribution in condensation polymers[20] and chain-length distribution in radical polymerization[21]. The simulation algorithm is simple and can be easily extended to deal with problems of high complexity. Mikes and Dušek[22] applied a Monte Carlo method, which is equivalent to kinetic theory of network formation, for simulation of stepwise polyreaction generating tree-like polymer structures. Recently, Netz and Samios[23] applied the Monte Carlo method to simulate network formation during the curing of an epoxy resin with anhydride and tertiary amine. They used a cluster–cluster aggregation model in which the reaction was modelled as a geometrical phenomenon and the chemical details were neglected.

In the present work, the network build-up in a diepoxide–anhydride system is simulated using the Monte Carlo technique in combination with the fragment approach of Riccardi and Williams[17]. Based on the kinetics of curing, various structural fragments present in the system are identified. The network generation is carried out by applying the Monte Carlo method to these structural fragments, keeping in view the principal reaction steps. An ideal case is assumed where all fragments combine randomly, independent of the state of neighbouring groups or the size of the molecule to which they are attached. The simulation takes into account the evolution of the network as a discrete and stochastic process. The method thus provides a detailed insight into the nature and composition of the network structure and enables calculation of structural parameters such as crosslink density, average weight between crosslinks as a function of conversion and also the chain-length distributions. These properties can be obtained easily by analysing the network once it is formed by the above simulation procedure.

The simulation procedure has been applied to tertiary-amine-initiated anhydride curing of diepoxide and compared with the fragment model in respect of only those average properties which can be calculated by both methods. Further characterization of the network has been done by calculating several structural parameters that are possible to evaluate only from a knowledge of the detailed network composition.

CONCEPT OF FRAGMENTS

Matějka *et al.*[24] have observed that reaction of epoxy

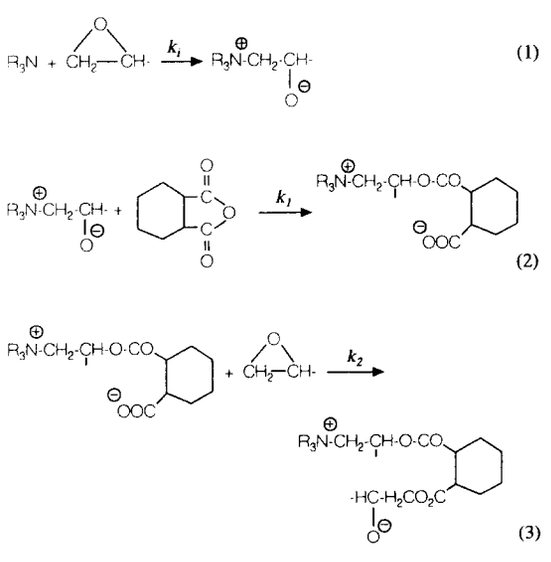

Figure 1 Reaction scheme of diepoxide curing with monoanhydride catalysed by tertiary amine

Table 1 Symbols and codes of the fragments for diepoxide–anhydride–tertiary amine curing system

Symbol	Code	Description	Mol. wt
◇	F_1	Unreacted tertiary amine	135
○→	F_2	Unreacted epoxy group	139
	F_3	Unreacted anhydride	154
	F_4	Alkoxide formed due to tertiary amine–epoxy reaction	274
	F_5	Reacted F_4	274
	F_6	Partially reacted anhydride with carboxylate end	154
	F_7	Completely reacted anhydride	154
	F_8	Alkoxide formed during propagation reaction	139
	F_9	Reacted F_8	139

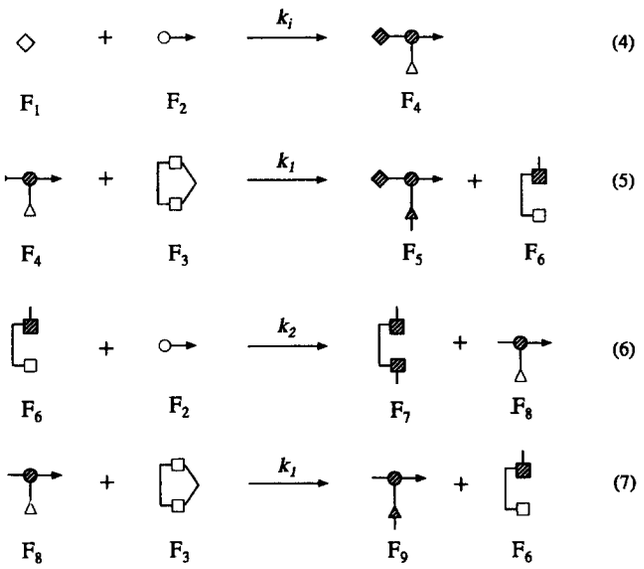

Figure 2 Reaction scheme in terms of fragments for a diepoxide–anhydride–tertiary amine curing system

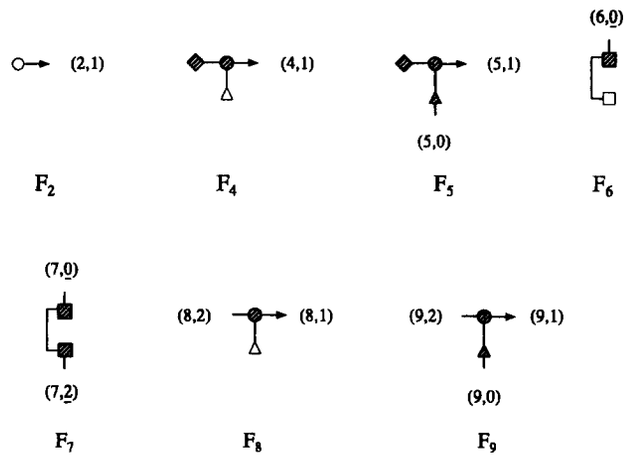

Figure 3 Labels for the link ends (arms) of the network fragments

compounds with acid anhydrides catalysed by tertiary amines takes place according to the scheme in *Figure 1* where k_i, k_1 and k_2 are the rate constants for the various reaction steps.

The reaction shown in equations (1)–(3) is depicted in terms of sub-units called fragments. The entire reaction system, comprising the monomers, catalyst and product, is represented in terms of these repeat units (fragments). The various combinations of these fragments are able to denote the unreacted species as well as the larger molecules emerging as a consequence of polymerization. Each fragment has linking arm(s) by which it can link to the other fragment(s). Corresponding to the reaction scheme shown in *Figure 1*, nine structural fragments

are present in a diepoxide–monoanhydride system, as shown in *Table 1*. In terms of these fragments, the reaction scheme of equations (1)–(3) is shown in *Figure 2*. The main assumption underlying the identification of fragments and subsequent model development is that the reactivities of all the epoxy groups on a molecule are the same and independent of each other. Equations (6) and (7) constitute the propagation reactions for the curing of an epoxy–anhydride system.

The reaction scheme shown in equations (4)–(7) indicates that, apart from fragments F_1 and F_3, all the other fragments can be a part of the network.

A fragment is represented by a number, j, and an arm of the fragment (also called a link end) is denoted by two numbers j and k. The number j can take any value from 1 to 9 corresponding, respectively, to the nine fragments F_1–F_9. Thus j refers to the kind of fragment. The number k, on the other hand, refers to the type of linkage. The various fragments along with the labels on their link ends are shown in *Figure 3*. Each link end is thus represented by two numbers; e.g. fragment F_9 (*Figure 3*) has three link ends represented by (9,0), (9,1) and (9,2).

The rule for connectivity is that only arms having the same k value have the potential to link together. For k values 0 and 2, an additional criterion for connectivity is to be satisfied, since having the same k value on the arms does not ensure that the fragments can link up through them. This follows from the fact that the fragment arms capable of joining together should also conform to the linkages formed by the reaction steps (4)–(7). The k values 0 and 2 are therefore further differentiated as 0, $\underline{0}$ and 2, $\underline{2}$, respectively. Thus 0 can only link to $\underline{0}$ and vice versa; similarly 2 can only link to $\underline{2}$ and vice versa. However, link ends having k value $\bar{1}$ connect to each other. Based on *Figure 3* and equations (4)–(7), the various options for connectivity of a fragment arm are shown in *Table 2*.

Considering reactions (4)–(7), the rate expressions for the various fragments can be written as:

$$\frac{dC_1}{dt} = k_1 C_1 C_2 \tag{8}$$

$$\frac{dC_2}{dt} = k_1 C_1 C_2 - k_2 C_2 C_6 \tag{9}$$

$$\frac{dC_3}{dt} = -k_1 C_3 (C_4 + C_8) \tag{10}$$

$$\frac{dC_4}{dt} = k_1 C_1 C_2 - k_1 C_3 C_4 \tag{11}$$

$$\frac{dC_5}{dt} = k_1 C_3 C_4 \tag{12}$$

$$\frac{dC_6}{dt} = k_1 C_3 (C_4 + C_8) - k_2 C_2 C_6 \tag{13}$$

$$\frac{dC_7}{dt} = k_2 C_2 C_6 \tag{14}$$

$$\frac{dC_8}{dt} = k_2 C_2 C_6 - k_1 C_3 C_8 \tag{15}$$

$$\frac{dC_9}{dt} = k_1 C_3 C_8 \tag{16}$$

where C_i ($i = 1, 2, \ldots, 9$) is the concentration of the ith fragment. Equations (8) to (16) comprise a set of coupled ordinary differential equations, which are solved numerically to obtain the concentration profiles of all the fragments. In the present work, the initial conditions and rate constants used are based on the data of Matějka *et al.*[24] for the curing of the phenyl glycidyl ether–benzoic acid anhydride system catalysed by benzyldimethylamine (BDMA). The curing system considered is isophthalic diglycidyl ester–hexahydrophthalic anhydride catalysed by BDMA, where the epoxy, anhydride and catalyst are in the molar ratio 1 : 1 : 0.15.

Table 2 Connectivity options for the various link ends

Link end	Options for linking
(4,1)[a]	(2,1), (4,1), (5,1), (8,1), (9,1)
(5,0)	(6,$\underline{0}$), (7,$\underline{0}$)
(6,$\underline{0}$)	(5,0), (9,0)
(7,$\underline{0}$)	(5,0), (9,0)
(7,$\underline{2}$)	(8,2), (9,2)
(8,2)	(7,$\underline{2}$)
(9,0)	(6,$\underline{0}$), (7,$\underline{0}$)
(9,2)	(7,$\underline{2}$)

[a] Same options for (2,1), (5,1), (8,1) and (9,1)

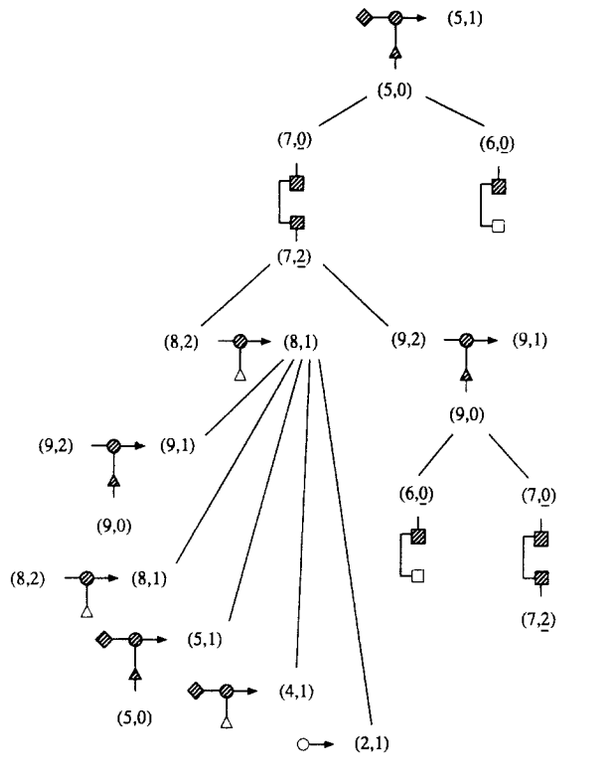

Figure 4 Schematic of simulation procedure starting from F_5 fragment with options for link ends shown at each step

SIMULATION MODEL

Since each polymer molecule begins with an F_5 fragment (equation (5)), the simulation starts from the F_5 fragment. This offers two link ends. For each link end, taken in succession, the various options are considered, as shown in *Figure 4*, and an appropriate fragment is chosen for linkage by the Monte Carlo method described below. As a linkage is established it leads to new link ends since the fragment chosen carries its own link ends

(of which only one is destroyed in forming the linkage). Thus the evolving network species now has a new set of link ends. Since the fragments F_2, F_4 and F_6 offer only one link end, they can become only the terminal units in any network.

The nature of the link end determines the various fragments that can attach to it. If there is more than one option for linkage, the fragment (for attachment) is chosen based on a uniformly distributed random variable X_1 according to the following relation:

$$\sum_{m=1}^{r-1} P_m < X_1 \leqslant \sum_{m=1}^{r} P_m \tag{17}$$

where P_m is the probability of the mth option ($m = 1, \ldots, N$; N being the total number of options for the link end under consideration). For the rth option to be selected, the random number X_1 should satisfy equation (17). P_m satisfies the normalization condition:

$$\sum_{m=1}^{N} P_m = 1 \tag{18}$$

The probability of the mth option, P_m, is given by the ratio of concentration of the fragment associated with the mth option to the sum of concentrations of all the fragments associated with the different linkage options for the given link end.

Considering the link end (7,2), for example, the linkage options available to it are (8,2) and (9,2). Therefore, the probabilities of the two options are:

$$P_1 = \frac{C_8}{C_8 + C_9} \quad \text{and} \quad P_2 = \frac{C_9}{C_8 + C_9}$$

where C_8 and C_9 are the concentrations of the fragments F_8 and F_9. If the random number X_1 lies between 0 and P_1, fragment F_8 is selected; otherwise, fragment F_9 is chosen. If F_8 is chosen, it destroys the link end (7,2) and replaces it by the new link end (8,1); whereas choosing F_9 leads to two new link ends (9,0) and (9,1). Considering further selection of fragments for the new link (8,1), there are five options as shown in *Figure 4*, viz. (2,1), (4,1), (5,1), (8,1) and (9,1). The probability for the first option is then:

$$P_1 = \frac{C_2}{C_2 + C_4 + C_5 + C_8 + C_9} \tag{19}$$

The probabilities for the other options are obtained similarly.

Simulation procedure

The first step in simulation involves converting the fragment concentrations from molar basis to molecules per unit volume. This can be done by multiplying the fragment concentration with Avogadro's number. Since the total number of molecules so obtained is too large to handle, the multiplying factor is reduced. Instead of using Avogadro's number, a scale factor is chosen such that further increase in the scale factor does not alter any chosen property of the polymerizing system. *Table 3* shows the effect of scale factor on weight-average molecular weight at pre-gel and post-gel conversions. For the present work a scale factor of 10^4 has been used. The number of molecules N_i of the ith fragment at any time is given by:

$$N_i = (\text{scale factor}) \times C_i \tag{20}$$

where C_i is the concentration of the ith fragment. The number of molecules of fragment i in the polymer molecule is denoted by N_{pi}. As the polymer molecule grows, N_{pi} increases with a corresponding decrease in N_i.

The simulation of each polymer molecule (or network species) commences with an F_5 fragment. This constitutes the first node of the network tree. Corresponding to each fragment, selected by the Monte Carlo method for attachment to the link end of a node, a new node is created in the network tree. The identity of the new node (I_N) is the same as that of the fragment chosen. The list of link ends (L) present on the tree is updated following each attachment.

The process of attaching fragments is continued till (a) there are no more link ends on any arm of the polymer molecule or (b) there are no more fragments available for linking. If case (a) is encountered and there are some F_5 or F_4 still remaining, the build-up of a new polymer molecule is started. The counter NP, denoting the number of polymer molecules present in the system, is incremented every time a new polymer molecule is built. For case (b), since the network itself contains unattached link ends, they are collapsed into each other. The mutual annihilation of link ends is carried out till there are no more link ends on the network. The criterion for collapsing link ends conforms to that shown in *Table 2*.

The molar mass of each polymer molecule generated is

Table 3 Variation of $\overline{M}_w$ and $(\overline{M}_c)_w$ with scale factor

x_e	Scale factor	$\overline{M}_w$	$(\overline{M}_c)_w$[a]
0.10	10^2	318	–
	10^3	324	–
	10^4	328	–
	10^5	325	–
0.20	10^2	753	–
	10^3	757	–
	10^4	758	–
	10^5	765	–
0.70	10^2	–	892
	10^3	–	1293
	10^4	–	1167
	10^5	–	1176
0.89	10^2	–	573
	10^3	–	523
	10^4	–	562
	10^5	–	577

[a] Weight-average molecular weight between crosslinks

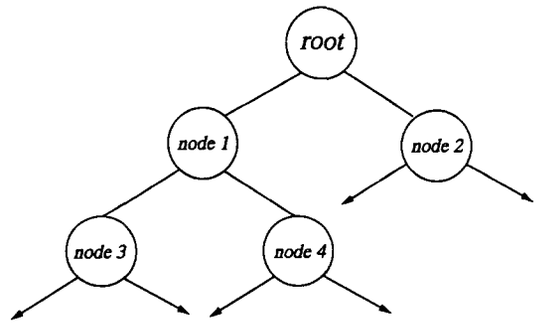

Figure 5 Typical structure of a network tree. An arrow (→) indicates continuation of network

calculated as:

$$\text{molar mass of polymer molecule} = \sum_{i=1}^{9} N_{pi} M_i \quad (21)$$

where M_i is the molar mass of the ith fragment.

A brief note regarding the data structures used will be in order before enumerating the simulation algorithm.

Data structures used in simulation

Network tree. The network structure is depicted in the form of a binary tree as shown in *Figure 5*. Each element of the network tree is called a node. A node can have one or two arms emanating from it, where each arm in turn leads to a node called the child node, e.g. nodes 3 and 4 are the children of node 1, which is therefore a parent node. Evidently each node is a parent as well as a child node. The tree starts from a node called the *root*, which is different from other nodes because it has no parent node. Since the simulation commences with the F_5 fragment, the root identity is fixed as 5. The identity of each node is denoted by I_N and that of its parent by I_P. Each node is also assigned a level depending on its distance from the root. The root is assigned level 0 and node 1 will therefore be at level 1, node 3 at level 2. A node in the network tree carries the following information: (a) its parent node; (b) node identity, I_N; (c) its child nodes; and (d) the level at which it occurs.

Link ends. During the simulation of each polymer molecule, all the link ends present on it are stored in a sequential list, L. Each element of this list contains the following information: (a) fragment to which the link end belongs (F_2, F_4, F_5, etc.), i.e. the j value; (b) nature of the link end (0, 0, 1, 2, 2), i.e. the k value; and (c) node in the network tree from which it emanates.

Algorithm

The steps of the simulation procedure are enumerated below:

1. Input the nine fragment concentrations (C_i), their molecular weights (M_i) and scale factor
2. Calculate the number of molecules of the ith fragment, N_i, using equation (20)
3. Initialize the number of polymer molecules, NP, to zero
4. Build polymer molecules from F_5 fragment
   (a) Increment NP by one
   (b) Initialize number of molecules of ith fragment in the polymer molecule, N_{pi}, to zero (where $i = 2, 4, 5, 6, 7, 8, 9$)
   (c) Depending on the root fragment, increment corresponding N_{pi} and decrease N_i by one
   (d) Initialize the network tree in the form of a binary tree structure by setting the root identity, I_N
   (e) Create list of link ends, L
   (f) Examine L and attach nodes to the network tree
      (i) for each link end (j,k) choose the fragment for attachment (*Table 2*)
      (ii) if the ith kind of fragment is chosen for attachment $N_i = N_i - 1$, $N_{pi} = N_{pi} + 1$
      (iii) create a new mode for the chosen fragment
         (1) set node identity, $I_N = i$
         (2) set its parent node identity $I_P = j$
         (3) assign appropriate level to the new node
         (4) attach the newly created node to the network tree
   (g) Update L based on the nodes attached
   (h) Check if L is empty
   (i) If no
      (i) check if unattached fragments are zero
      (ii) if no, go to step 4(f)
      (iii) if yes, collapse the network tree ends
         (1) for a link end in L, choose appropriate link end (*Table 2*) for collapsing
         (2) scan L till the desired link end is found
         (3) make appropriate connection in the network tree for the above two link ends
         (4) remove both the link ends from L
         (5) check if L is empty
         (6) if not, go to step 4(i)(iii)(1)
         (7) if yes, go to step 4(j)
   (j) If yes
      (i) calculate molar mass of polymer molecule (equation (21))
      (ii) identify the crosslinks in the polymer molecule (described later)
      (iii) find all the elastically active network chains (described later)
5. Check if N_5 is zero
   (a) If no, check if unattached fragments are zero
      (i) if no, go to step 4
      (ii) if yes, go to step 6
   (b) If yes, go to step 7
6. Calculate
   (a) Sol fraction
   (b) Elastic fraction
   (c) Pendent fraction
7. Stop

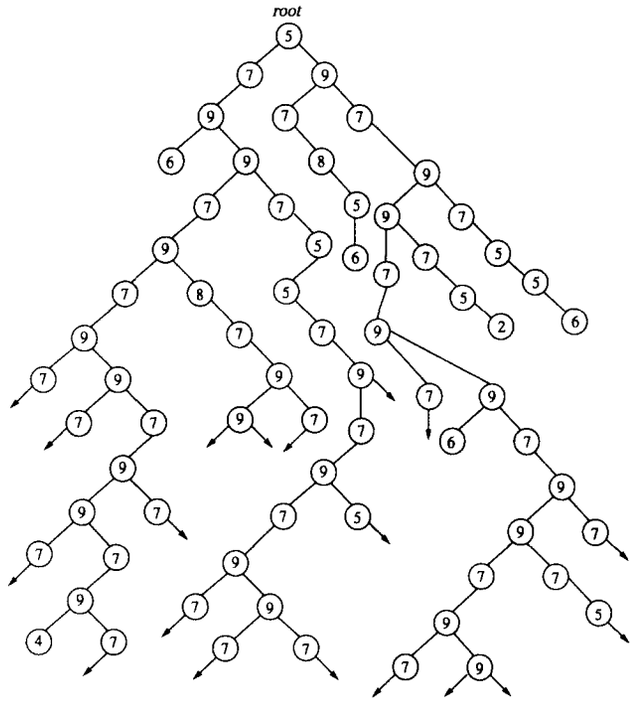

Figure 6 Portion of the simulated network tree at epoxy conversion 0.8, using a scale factor of 100. An arrow (→) indicates continuation of network

Figure 6 shows a part of the simulated network tree using a scale factor of 100 for the epoxy conversion of 80%.

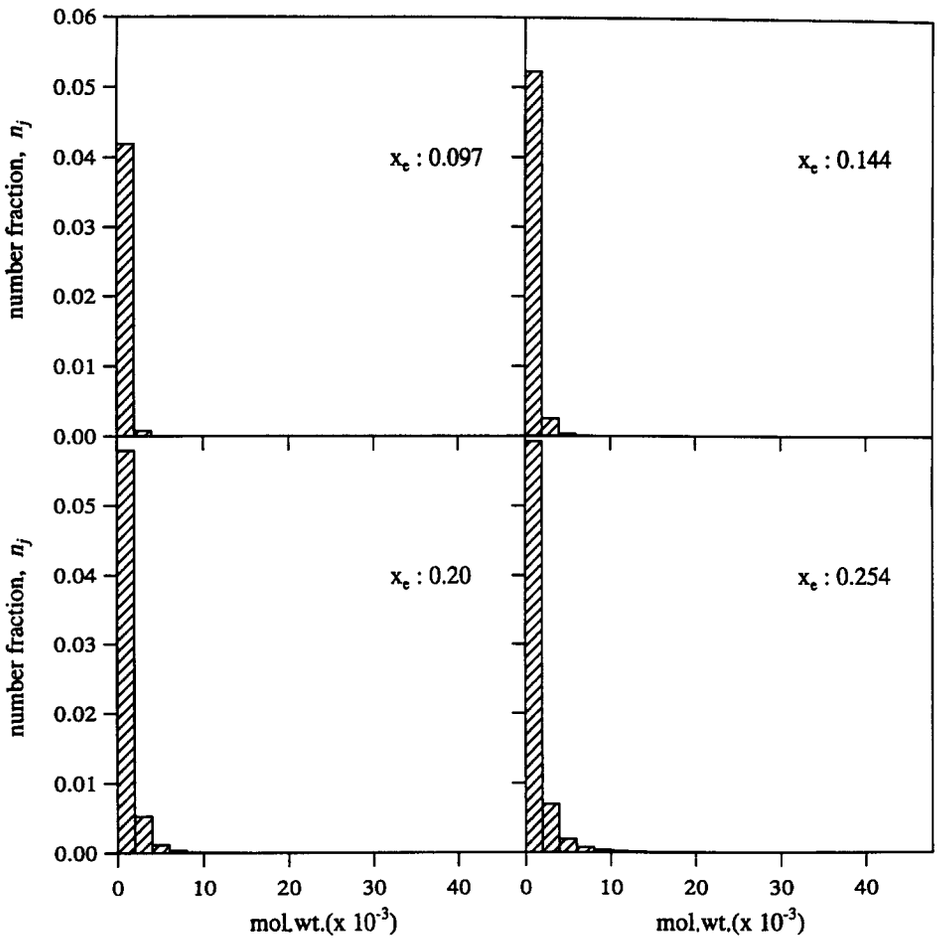

Figure 7 Molecular-weight distribution (number fraction) of reaction products obtained by simulation at different levels of epoxy conversion (x_e)

RESULTS AND DISCUSSION

Average molecular weight

At any time during the course of reaction, simulation gives the number of all the polymer molecules of different molecular weights. The number and weight distribution of all the molecular species can be evaluated by calculating the mole fraction $n_j = N_j/N$ and weight fraction $w_j = W_j/W$, where N_j is the number of moles and W_j is the weight of the jth species; $N = \sum_j N_j$ and $W = \sum_j W_j$. The number- and weight-distribution curves are shown in *Figures 7* and *8*, respectively. As epoxy conversion increases, larger-molecular-weight species start emerging (*Figure 8*) accompanied by a significant decrease in the weight fraction of lower-molecular-weight species. On the other hand, these high-molecular-weight polymer molecules, being small in number, do not exhibit a significant change in the number fraction histograms and the number fraction of the smaller species still dominates (*Figure 7*).

The number-average molecular weight $\overline{M}_n$ and the weight-average molecular weight $\overline{M}_w$ can be calculated from:

$$\overline{M}_n = \sum_j n_n M_j \tag{22}$$

and

$$\overline{M}_w = \sum_j w_j M_j \tag{23}$$

where M_j is the molecular weight of the jth species.

Since in epoxy curing the total mass of the system does not change with time, it can be expressed in terms of the initial concentration of the reactants ($c_{1,0}, C_{2,0}, C_{3,0}$) as:

$$\text{total mass} = C_{1,0}M_1 + C_{2,0}M_2 + C_{3,0}M_3 \tag{24}$$

The reaction scheme described by equations (1)–(3) shows that, every time an epoxy or anhydride reacts, the number of moles diminishes by one unit. Therefore the total moles at any time t can be expressed in terms of the initial concentration of the reactants and the extent of reaction:

$$\text{total moles at any time } t = C_{1,0} + C_{2,0}/2 + C_{3,0} - x_e C_{2,0} - x_a C_{3,0} \tag{25}$$

where x_e and x_a represent the conversion of epoxy and anhydride groups, respectively.

The anhydride is consumed only by the reaction with alkoxide, whereas epoxy is consumed by two reactions, namely the reaction with tertiary amine (equation (1)) and reaction with carboxylate (equation (3)). Since the amount of epoxy consumed in the first reaction (equation (1)) is usually negligible compared to that consumed in the second (equation (3)), we can use the approximation $x_e \approx x_a$. Substituting this along with equations (24) and (25) in equation (22), $\overline{M}_n$ is given by:

$$\overline{M}_n = \frac{C_{1,0}M_1 + C_{2,0}M_2 + C_{3,0}M_3}{C_{1,0} + C_{2,0}/2 + C_{3,0} - 2x_e C_{2,0}} = \frac{r_1 M_1 + M_2 + r_3 M_3}{r_1 + 0.5 + r_3 - 2x_e} \tag{26}$$

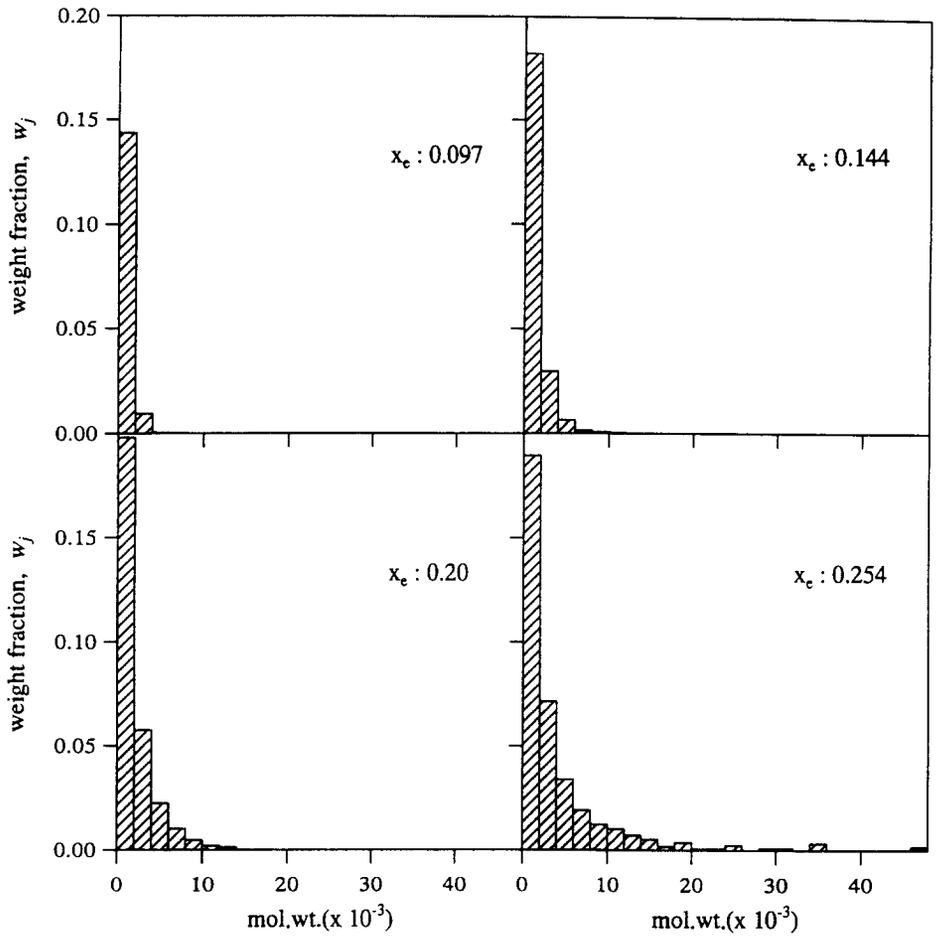

Figure 8 Molecular-weight distribution (weight fraction) of reaction products obtained by simulation at different levels of epoxy conversion (x_e)

where $r_1 = C_{1,0}/C_{2,0}$ and $r_3 = C_{3,0}/C_{2,0}$. Therefore the variations in $\overline{M}_n$ with epoxy conversion can be predicted from the initial reactant concentrations.

Riccardi[17] applied expectation theory and predicted weight-average molecular weight, sol fraction, etc., for an epoxy–amine system. Using a similar approach to calculate $\overline{M}_w$, we can define average weights attached to the different linking ends. Let A_0, $A_{\underline{0}}$, A_1, A_2 and $A_{\underline{2}}$ be the average weights hanging from (0), ($\underline{0}$), (1), (2) and ($\underline{2}$), respectively. According to the expectation theory, the expected value of a discrete random variable Y, denoted by $E(Y)$, is given by:

$$E(Y) = \sum_{\text{all } y} y f(y) \tag{27}$$

where $f(y)$ is the density function and y is the value of the random variable Y. The average weight hanging from link ends of type (1) can thus be written as:

$$A_1 = \sum_{\text{all fragments}} y f(y) \tag{28}$$

where

y = average weight hanging from a given (1)

$f(y)$ = probability of finding the (1) on the fragment

$$= \frac{\text{number of (1) on the fragment}}{\text{total number of (1)}}$$

Thus:

$A_1 = \sum_{\text{all fragments}}$ [average weight hanging from the (1) on the fragment]

× [fraction of total (1) associated with the fragment]

$$= \frac{1}{C_{2,0}}[C_2M_2 + C_4M_4 + C_5(M_5 + A_0) + C_8(M_8 + A_2) + C_9(M_9 + A_0 + A_2)] \tag{29}$$

Similarly A_0, $A_{\underline{0}}$, A_2 and $A_{\underline{2}}$ can be defined as:

$$A_0 = \frac{C_6M_6 + C_7(M_7 + A_{\underline{2}})}{C_6 + C_7} \tag{30}$$

$$A_{\underline{0}} = \frac{C_5(M_5 + A_1) + C_9(M_9 + A_2 + A_1)}{C_5 + C_9} \tag{31}$$

$$A_2 = \frac{C_7(M_7 + A_{\underline{0}})}{C_7} \tag{32}$$

$$A_{\underline{2}} = \frac{C_8(M_8 + A_1) + C_9(M_9 + A_1 + A_0)}{C_8 + C_9} \tag{33}$$

As a consequence of the connectivity rules, the number of link ends of type (0), ($\underline{0}$), (2) and ($\underline{2}$) must be balanced. Thus:

$$C_5 + C_9 = C_7 + C_6 \tag{34}$$

$$C_7 = C_8 + C_9 \tag{35}$$

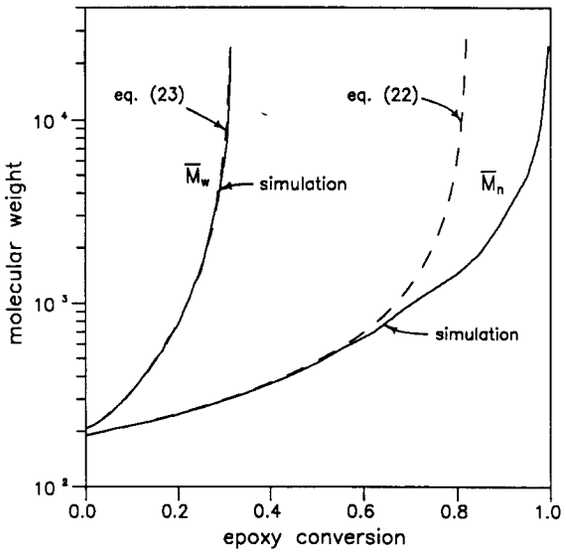

Figure 9 Variation of $\overline{M}_w$ and $\overline{M}_n$ with epoxy conversion: a comparison between simulation and fragment model

Using equations (34) and (35), equations (30) and (33) can then be written as:

$$A_0 = \frac{C_6M_6 + C_7(M_7 + A_2)}{C_5 + C_9} \tag{36}$$

$$A_{\underline{2}} = \frac{C_8(M_8 + A_1) + C_9(M_9 + A_1 + A_0)}{C_7} \tag{37}$$

Equations (29), (31), (32), (36) and (37) are solved numerically for A_1, A_0, $A_{\underline{0}}$, A_2 and $A_{\underline{2}}$. The weight-average molecular weight is defined as:

$$\overline{M}_w = \sum_{i=1}^{9} W_i M_{Ti} \tag{38}$$

where

$$W_i = \text{weight fraction of } i\text{th fragment} = \frac{C_iM_i}{C_{1,0}M_1 + C_{2,0}M_2 + C_{3,0}M_3}$$

$$M_{Ti} = \text{average weight of the } i\text{th fragment} \tag{39}$$

The expressions for M_{Ti} for the different fragments are:

$$\begin{aligned} M_{T1} &= M_1 \\ M_{T2} &= M_2 + A_1 \\ M_{T3} &= M_3 \\ M_{T4} &= M_4 + A_1 \\ M_{T5} &= M_5 + A_1 + A_0 \\ M_{T6} &= M_6 + A_{\underline{0}} \\ M_{T7} &= M_7 + A_{\underline{0}} + A_{\underline{2}} \\ M_{T8} &= M_8 + A_1 + A_2 \\ M_{T9} &= M_9 + A_1 + A_0 + A_2 \end{aligned} \tag{40}$$

Using the values of A_1, A_0, $A_{\underline{0}}$, A_2 and $A_{\underline{2}}$ obtained from equations (29), (30), (32), (36) and (37), the average weight of each fragment can be calculated from equation (40). Substituting these in equation (38), the weight-average molecular weight $\overline{M}_w$ can be predicted as a function of epoxy conversion.

Figure 9 shows a comparison between the average molecular weights predicted by equations (26) and (38) with the corresponding values obtained by simulation.

Gel point

As the reaction proceeds, larger species are built up at the expense of the smaller ones. An infinite network forms at the gel point and its weight fraction rapidly increases. Simulation results, shown in *Figure 9*, indicate that the gel point occurs around 30% conversion. Equation (40) shows that $\overline{M}_w$, given by equation (38), is a function of A_1, A_0, $A_{\underline{0}}$, A_2 and $A_{\underline{2}}$. Thus, the gel condition, where $\overline{M}_w \to \infty$, occurs when A_1, A_0, $A_{\underline{0}}$, A_2 and $A_{\underline{2}} \to \infty$.

Substituting equation (36) into equation (37) and simplifying, we obtain:

$$A_0 = \frac{C_6M_6 + C_7M_7 + C_8M_8 + C_9M_9 + A_1(C_8 + C_9)}{C_5} \tag{41}$$

Similarly from equations (31) and (32):

$$A_2 = \frac{M_7(C_5 + C_9) + C_5M_5 + C_9M_9 + A_1(C_5 + C_9)}{C_5} \tag{42}$$

Thus A_0 and A_2 can be expressed as functions of A_1 only. It then follows from equations (31) and (33) that $A_{\underline{0}}$ and $A_{\underline{2}}$ also can be expressed as functions of A_1 only.

Hence the gel condition can be simply stated as $A_1 \to \infty$.

Substituting equations (41) and (42), equation (29) may be rearranged to the form:

$$A_1 = \frac{K_1 + K_2}{C_{2,0} - 2(C_7/C_5)(C_5 + C_9)} \tag{43}$$

where

$$K_1 = C_2M_2 + C_4M_4 + C_5M_5 + C_8M_8 + C_9M_9$$

and

$$K_2 = (C_6M_6 + C_7M_8 + C_8M_8 + C_9M_9)(C_5 + C_9)/C_5 + [M_7(C_5 + C_9) + C_5M_5 + C_9M_9]C_7/C_5$$

The condition for $A_1 \to \infty$ is then given by:

$$C_{2,0} = 2(C_7/C_5)(C_5 + C_9) \tag{44}$$

This is the gel condition according to the fragment model for the present system and is seen to be satisfied at about 32% epoxy conversion. *Figure 9* shows this to be in good agreement with the gel conversion obtained by simulation.

It is seen from *Figure 9* that, according to simulation results, $\overline{M}_n$ tends to infinity at about 90% conversion, while according to equation (26), $\overline{M}_n \to \infty$ at about 80% conversion. This difference arises because equation (26) assumes that each time an epoxy group reacts the number of moles diminish by one and thus excludes the possibility of the cyclization reactions. However, this condition is not satisfied especially in the later stages of network growth, owing to the possibility of intramolecular reactions (loop formation and cyclization), leading

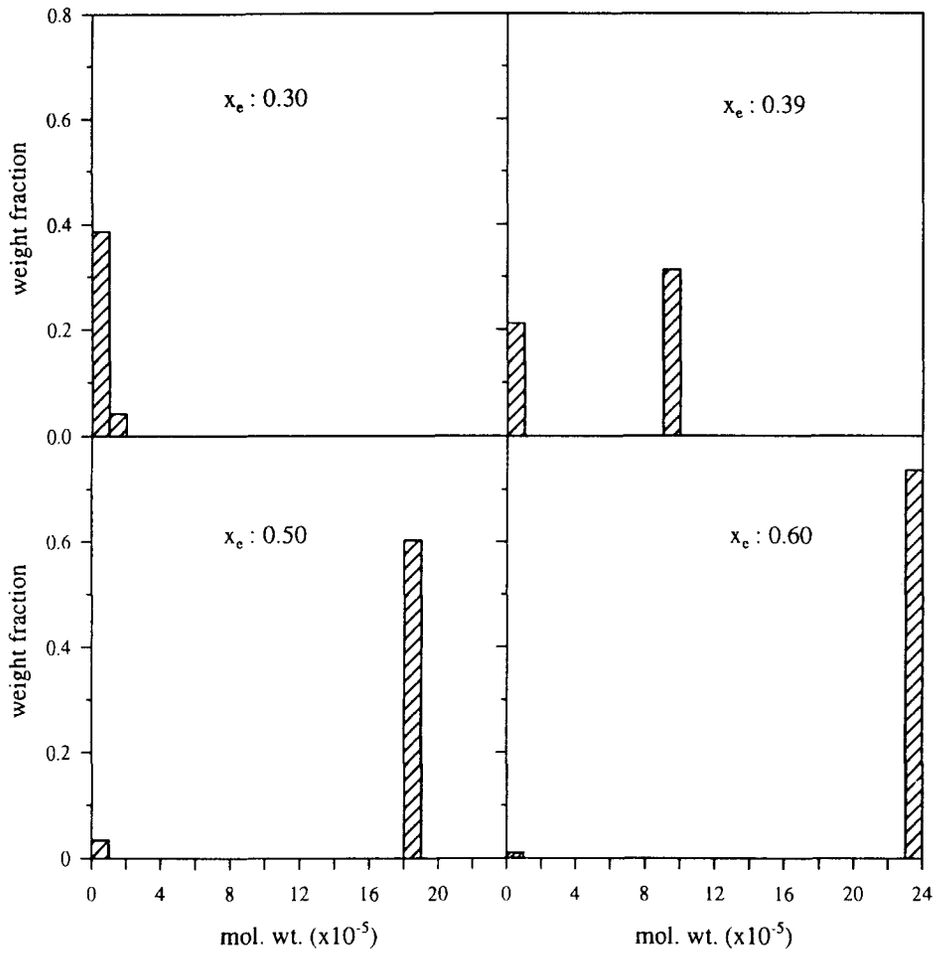

Figure 10 Molecular-weight distribution (weight fraction) of reaction products obtained by simulation at different levels of epoxy conversion (x_e) beyond gel point

to a less rapid reduction in moles of discrete species with increasing epoxy conversion. The calculated number-average molecular weight according to simulation thus tends to infinity at a later stage of conversion than that predicted by equation (26).

Continuing the simulation beyond the gel point, the amount of gel is found to increase at the expense of the smaller species till a single large macromolecule emerges. Simulation results show that the various polymeric products that appear, as the conversion increases, merge into the single macromolecule at a conversion of around 60% (*Figure 10*). At this conversion level the reaction system comprises only a single macromolecule besides the unreacted monomer species.

Crosslink density

A node or branch point is considered as a crosslink point if at least three of its arms or branches lead into the network. In practical terms, a branch may be considered to be leading into the network if, by moving along its path, through an *infinite* number of fragments, one never encounters an end or terminal unit. For the simulated network of finite size, this infinite number is substituted by a definite number of fragments that must be attached to all three arms (nodal branches) to categorize the node as a crosslink point. This number is such that consideration of a still larger number of fragments on the nodal branch does not lead to a significant change in the computed value of network parameters like crosslink concentration.

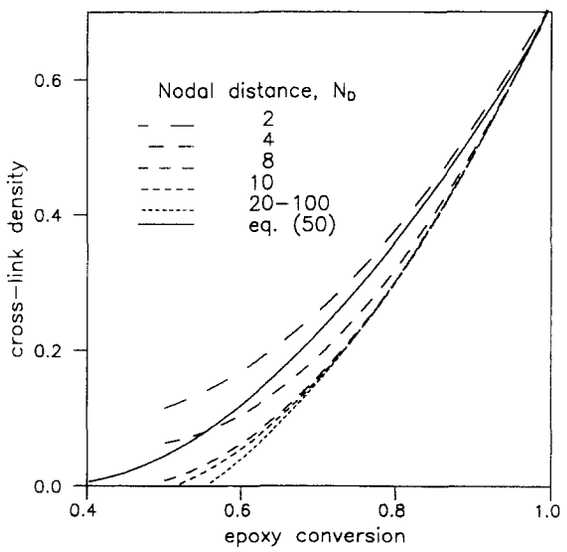

Figure 11 Variation of crosslink density with epoxy conversion obtained by simulation, for different nodal distances (N_D)

In order to mark the crosslink point in the simulated network, fragments that offer at least three arms are first identified. For the epoxy–anhydride system under

consideration, only F_9 satisfies this condition. If none of the three arms of F_9 ends in a terminal unit while scanning over a certain distance from the node, F_9 is classified as a crosslink point. As explained earlier, only the fragments F_2, F_4 and F_6 can be the terminal units in a network. Therefore, for an F_9 fragment to be considered as a crosslink point, none of its three arms should feature any of the fragments F_2, F_4 and F_6 within the specified distance from the node, considering, however, all possible paths an arm can lead to. The distance to be scanned is specified in terms of the number of fragments present on the arm, starting from F_9, and is designated as a nodal distance N_D. The crosslink concentration as a function of epoxy conversion for varying values of N_D is shown in *Figure 11*.

It is seen that the crosslink concentration in a network at any given conversion decreases with the increase in N_D. However, the crosslink concentration, which decreases more rapidly at low values of N_D, becomes nearly constant when the value of N_D exceeds 20. This can be explained as follows. A branch emanating from an F_9 node terminates in a free end only when it adds to one of the terminal units F_2, F_4 or F_6. Matějka *et al.*[24] have observed that the concentration of tertiary amine drops very rapidly in the initial phase of reaction with a corresponding increase in the carboxylate species. The concentration of the carboxylate species then remains almost constant throughout the reaction period. This implies that after the initial reaction phase the concentration of F_6 (carboxylate species) and F_4 (initiating species) can be considered as constant and hence will not have much effect on the variation of crosslink concentration with nodal distance. On the other hand, the concentration of F_2 (unreacted epoxy group) decreases with conversion and is very small even at moderately high conversions. The frequency of occurrence of F_2 on the network thus drops to almost zero at some distances from the root node F_5 and the crosslink concentration then becomes nearly independent of the nodal distance

The algorithm to identify an F_9 fragment as a crosslink point is enumerated below. The network tree is scanned and each node is examined for a potential crosslink point.

1. Input the nodal distance, N_D
2. Check if node identity, I_N, is 9
3. If yes
   (a) Initialize flags for left and right arms, Lflag = Rflag = 0
   (b) Set level = node level + N_D
   (c) Check the left arm and right arm for N_D reacted fragments recursively. The identity of nodes on all the possible paths on each arm is checked.
      (i) check I_N for the node
      (ii) if $I_N \neq 2$, 4 or 6 and node level < level, go to step 3(c)(i)

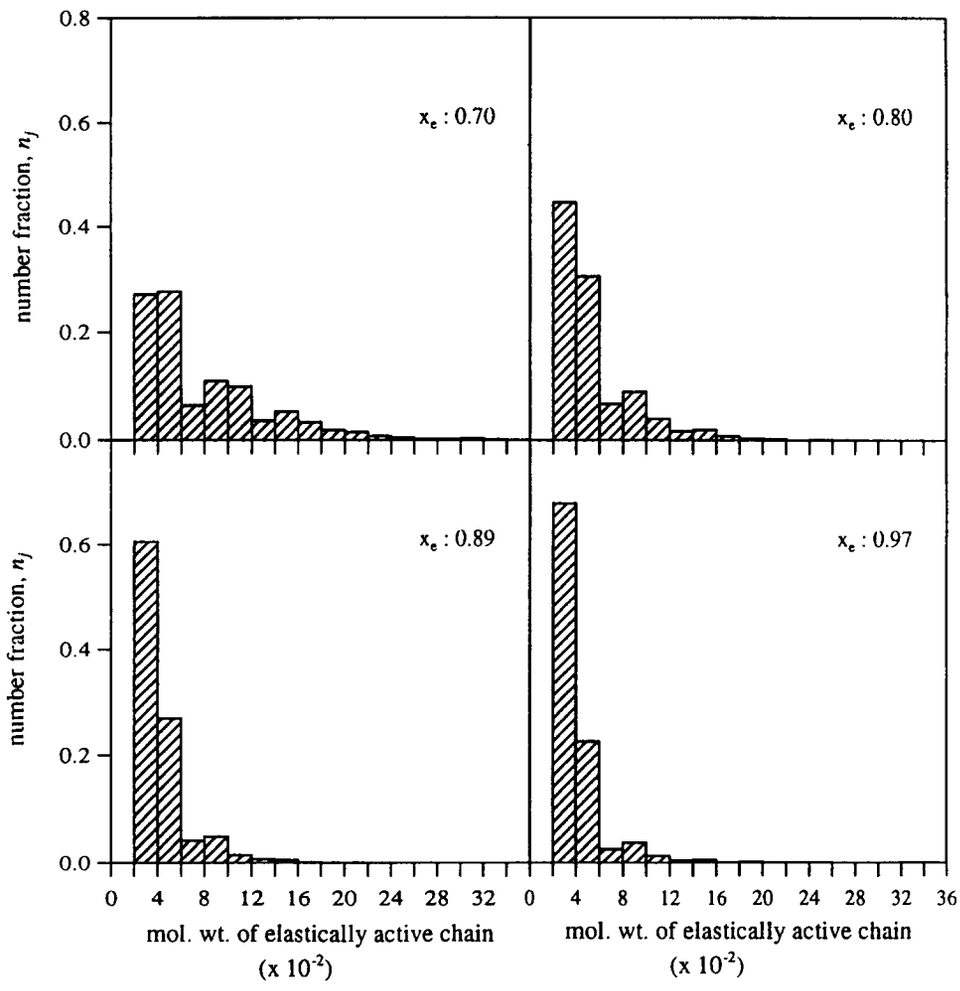

Figure 12 Molecular-weight distribution of EANCs (number fraction) in the simulated network at different levels of epoxy conversion (x_e)

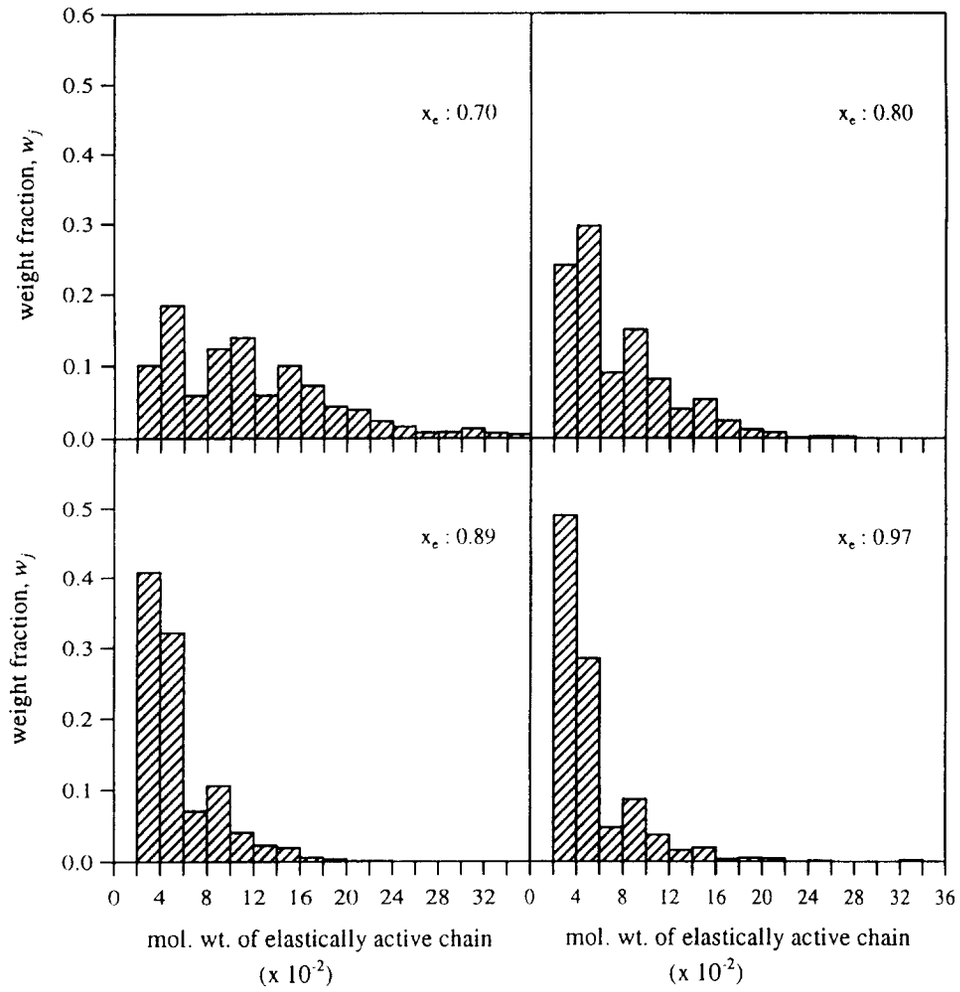

Figure 13 Molecular-weight distribution of EANCs (weight fraction) in the simulated network at different levels of epoxy conversion (x_e)

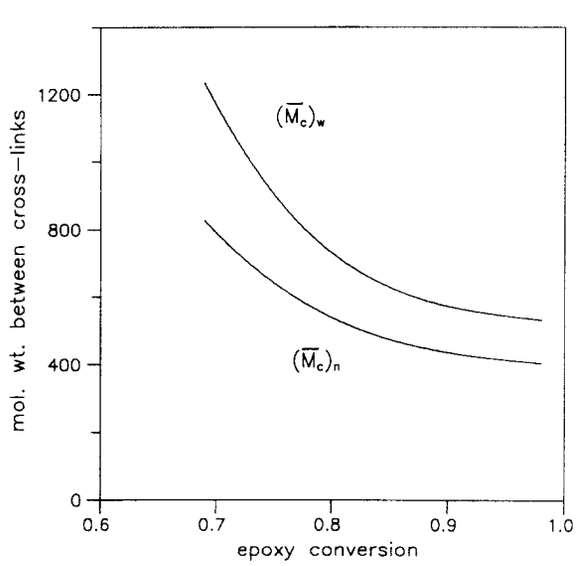

Figure 14 Variation of average molecular weight between crosslinks in the simulated network as a function of epoxy conversion

(iii) if $I_N = 2$, 4 or 6 and node level < level, go to step 3(c)(i) with the other child node
(iv) if $I_N \neq 2$, 4 or 6 and node level = level, set the appropriate flat (Lflag or Rflag) to one

(d) If Lflag = 1 and Rflag = 1, the node is a crosslink

4. If no
   (a) Set node as the left child node and go to step 2
   (b) Set node as the right child node and go to step 2

Elastically active network chains

A chain segment embedded between two crosslink points constitutes an elastically active network chain (EANC). Once all the crosslink points in a network have been identified, finding EANCs becomes an easy task. The algorithm is enumerated below.

1. Starting from the root, note the path to each crosslink point in terms of the nodes encountered
2. Each and every possible combination of two paths is compared. For each comparison
   (a) Eliminate the nodes common to the paths
   (b) Check if, in the remaining portion of each path, a crosslink occurs
      (i) if yes, discard the comparison
      (ii) if no, the sum of the nodes in the remaining paths is the distance between the crosslinks
   (c) Calculate the molar mass of the elastic chain

While analysing the simulated network for EANCs, some loop formation was observed, i.e. the network chains started and ended at the crosslink point. Such loops do not contribute to the elastically active network chains, though their formation is more in accordance

with the real situation. The existing models ignore loop formation for the sake of simplicity.

The number and weight distributions of these chains are computed by calculating n_j and w_j where j refers to elastically active chains having the same molar mass. *Figures 12* and *13* show the number and weight distributions for the EANCs. The number-average molecular weight between crosslinks $(\overline{M}_c)_n$ and the weight-average molecular weight between crosslinks $(\overline{M}_c)_w$ are then calculated using equations (22) and (23) and plotted as a function of epoxy conversion in *Figure 14*. Higher conversions imply greater crosslinking and hence smaller chains between crosslinks. Thus both $(\overline{M}_c)_n$ and $(\overline{M}_c)_w$ decrease with increasing conversions. This is, however, observable only after a single large macromolecule has been formed in the system.

The crosslink density can also be calculated based on extinction probabilities[17], i.e. probability that a link end is connected to a finite chain. Let E_1, E_0, $E_{\underline{0}}$, E_2 and $E_{\underline{2}}$ be the extinction probabilities for the link ends (1), (0), ($\underline{0}$), (2) and ($\underline{2}$):

$$E_1 = \frac{C_2 + C_4 + C_5E_0 + C_8E_2 + C_9E_0E_2}{C_{2,0}} \quad (45)$$

$$E_0 = \frac{C_6 + C_7E_{\underline{2}}}{C_6 + C_7} \quad (46)$$

$$E_0 = \frac{C_5E_1 + C_9E_1E_2}{C_5 + C_9} \quad (47)$$

$$E_2 = \frac{C_7E_{\underline{0}}}{C_7} \quad (48)$$

$$E_{\underline{2}} = \frac{C_8E_1 + C_9E_1E_0}{C_8 + C_9} \quad (49)$$

Equations (45)–(49) are solved for the extinction probabilities. The crosslink density, defined as the moles of crosslink points per initial epoxy equivalent, is given by:

$$\text{crosslink density} = \frac{C_9(1 - E_1)(1 - E_0)(1 - E_2)}{C_{2,0}} \quad (50)$$

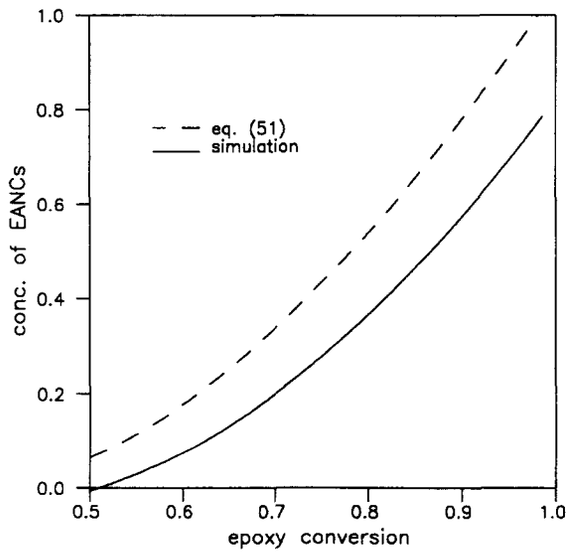

Figure 15 Concentration of EANCs as a function of epoxy conversion: comparison between the simulation and fragment model

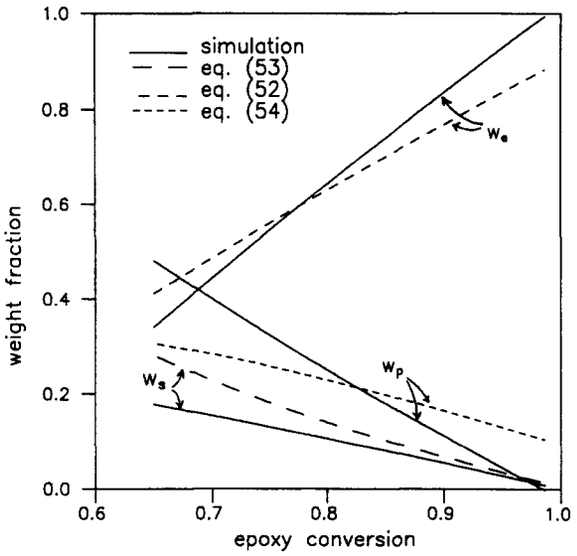

Figure 16 Plot of the sol, elastic and pendent weight fractions as a function of epoxy conversion

and the concentration of EANCs per initial epoxy equivalent is given by:

$$\text{concentration of EANCs} = (3/2) \times \text{crosslink density} \quad (51)$$

Figure 15 compares the concentration of EANCs obtained by simulation with that predicted by equation (51).

Sol and elastic fraction

As the conversion increases, the reaction system witnesses the emergence of high-molecular-weight species. Beyond a conversion of about 60%, there emerges a macromolecule having a molar mass much larger than any other species. The sol fraction is calculated only after this point is reached. For this calculation, the large macromolecule is considered as the insoluble fraction, with the remaining species constituting the sol fraction, w_s. Since the number of moles and molar mass of all the EANCs occurring in this macromolecule are known, the elastic fraction w_e is easily computed. The pendent fraction is calculated as:

$$w_p = 1 - w_s - w_e \quad (52)$$

The extinction probabilities, computed from equations (45)–(49), are also used to calculate the sol fraction and pendent fraction:

$$w_s = W_1 + W_2E_1 + W_3 + W_4E_1 + W_5E_1E_0 + W_6E_0 + W_7E_{\underline{0}}E_{\underline{2}} + W_8E_1E_2 + W_9E_1E_2E_0 \quad (53)$$

$$w_p = W_2(1 - E_1) + W_4(1 - E_1) + W_5[E_1(1 - E_0) + E_0(1 - E_1)] + W_6(1 - E_{\underline{0}}) + W_7[E_{\underline{0}}(1 - E_{\underline{2}}) + E_{\underline{2}}(1 - E_{\underline{0}})] + W_8[E_1(1 - E_2) + E_2(1 - E_1)] + W_9[E_1E_2(1 - E_0) + E_1E_0(1 - E_2) + E_2E_0(1 - E_1)] \quad (54)$$

The sol, elastic and pendent fractions obtained by

simulation are compared with those predicted by equations (52)–(54) in *Figure 16*.

CONCLUSIONS

A Monte Carlo method for simulation of curing in epoxy–anhydride–tertiary amine systems has been developed. The curing system has been identified in terms of repeat units called fragments. The simulation procedure involves the application of the Monte Carlo method to the arrangement of these fragments in the curing system. It enables visualization of the entire polymer network and evaluation of its characteristic properties. The simulation method has been applied to a diepoxide–monoanhydride system catalysed by tertiary amine where the epoxy, anhydride and tertiary amine are taken in the molar ratio 1 : 1 : 0.15. Pre-gel properties like the number and weight distributions, $\overline{M}_n$, $\overline{M}_w$, and critical conversion at the gel point are evaluated. After the onset of gelation, at around 30% conversion of epoxy groups, simulation results show the emergence of certain polymer species with very large molecular weights. These species merge into a single large macromolecule at nearly 60% conversion. The network properties, like concentration of crosslinks, number and weight distribution of elastically active chains (EANCs), concentration of EANCs and average molecular weight between crosslinks, have been evaluated after this point. The sol, pendent and elastic fractions have also been calculated. A comparison has been made in respect of some of these properties which can also be calculated independently from the fragment model. Good agreement has been observed in pre-gel properties like weight-average molecular weight and gel point, while for post-gel properties a significant difference is observed. This may be attributed largely to the fact that the Monte Carlo procedure developed in the present work permits intramolecular reactions leading to the formation of loops and other cyclic structures, while the fragment model rules out all such possibilities.

ACKNOWLEDGEMENT

We are grateful to the Council of Scientific and Industrial Research, India, for the award of a Research Scholarship to one of us (Umang Khanna).

REFERENCES

1 Flory, P. J. *J. Am. Chem. Soc.* 1941, **63**, 3083; 'Principles of Polymer Chemistry', Cornell University Press, Ithaca, NY, 1953, Ch. 9
2 Stockmayer, W. H. *J. Chem. Phys.* 1943, **11**, 45; 1944, **12**, 125
3 Stockmayer, W. H. *J. Polym. Sci.* 1952, **9**, 69; 1953, **11**, 424
4 Gordon, M. *Proc. R. Soc. Lond. (A)* 1962, **268**, 240
5 Harris, T. E. 'Theory of Branching Processes', Springer-Verlag, Berlin, 1963, Ch. 1
6 Malcolm, G. N. and Gordon, M. *Proc. R. Soc. Lond. (A)* 1966, **295**, 29
7 Dobson, G. R. and Gordon, M. *J. Chem. Phys.* 1965, **43**, 705
8 Gordon, M. and Parker, T. G. *Proc. R. Soc. Edinb. (A)* 1970/71, **69**, 13
9 Gordon, M., Ward, T. C. and Whitney, R. S. 'Polymer Networks' (Eds A. J. Chompf and S. Newman), Plenum Press, New York, 1971
10 Dušek, K., Gordon, M. and Ross-Murphy, S. B. *Macromolecules* 1978, **11**, 263
11 Dušek, K., Ilavaský, M. and Luňák, S. *J. Appl. Polym. Sci., Symp.* 1975, **53**, 29
12 Gordon, M. and Scantlebury, G. R. *Trans. Faraday Soc.* 1967, 1
13 Macosko, C. W. and Miller, D. R. *Macromolecules* 1976, **9**, 2
14 Bokare, U. M. and Gandhi, K. S. *J. Polym. Sci., Polym. Chem. Edn.* 1985, **18**, 857
15 Dušek, K. *Polym. Bull.* 1985, **13**, 321
16 Dušek, K. and Šomvársky, J. *Polym. Bull.* 1985, **13**, 313
17 Riccardi, C. C. and Williams, R. J. J. *Polymer* 1986, **27**, 913
18 Binder, K. (Ed.) 'Monte Carlo Methods in Statistical Physics', 2nd Edn., Topics in Current Physics, Vol. 7, Springer, Berlin, 1986
19 Gillespie, D. T. *J. Phys. Chem.* 1979, **81**, 2340
20 Yang, Y., Yu, T. and Tang, A. *Sci. Sin., Ser. B (English Edn)* 1988, **31**, 1418
21 Lu, J., Zhang, H. and Yang, Y. *Makromol. Chem., Theory Simul.* 1993, **2**, 747
22 Mikes, J. and Dušek, K. *Macromolecules* 1982, **15**, 93
23 Ntz, P. A. and Samios, D. *Macromol. Chem., Theory Simul.* 1994, **3**, 607
24 Matějka, L., Lövy, J., Pokorný, S., Bouchal, K. and Dušek, K. *J. Polym. Sci., Polym. Chem. Edn.* 1983, **21**, 2873